International Journal of Thermophysics, Vol. 19, No. 2, 1998

Simultaneous Measurement of Thermophysical and Mechanical Properties of Thin Films[1]

J. L. Hostetler,[2] A. N. Smith,[2] and P. M. Norris[2, 3]

Thermophysical and mechanical properties of thin films are investigated using ultrashort laser pulses (200 fs), which upon incidence create a temperature rise and generate an ultrasonic wave at the sample surface. By monitoring the thin film's reflectivity response after the deposition of radiation energy, the bulk modulus and thermal diffusivity normal to the surface can be extrapolated from a single data set. The resulting data show cooling profiles that vary greatly from the well-known Fourier diffusion model and agree favorably with the parabolic two-step heat diffusion model. This method can also be used to characterize electron–lattice energy coupling phenomena. Experimental results from bulk samples of copper and platinum as well as thin-film platinum were utilized to determine the values of the thermal diffusivity, bulk modulus, and electron-phonon coupling factor. In addition, the thin film platinum samples were studied with two substrates, silicon and glass, to gain more knowledge of the substrate's effect on transport properties.

KEY WORDS: bulk modulus; electron-phonon coupling factor; nonequilibrium heating; platinum; thermal diffusivity; thin films.

1. INTRODUCTION

Devices in the microelectronics industry have been fabricated with length scales of the order of tens of nanometers, where the reduction of the electron transit time plays a large role in the device's ability to perform tasks more quickly and efficiently. However, when size scales reach such short

[1] Paper presented at the Thirteenth Symposium on Thermophysical Properties, June 22-27, 1997, Boulder, Colorado, U.S.A.

[2] Department of Mechanical, Aerospace and Nuclear Engineering, University of Virginia, Charlottesville, Virginia 22903, U.S.A.

[3] To whom correspondence should be addressed.

0195-928X/98/0300-0569$15.00/0 © 1998 Plenum Publishing Corporation

dimensions, thermophysical and mechanical properties can be adversely affected and can degrade the performance of such devices by inhibiting the transfer of thermal and acoustic energy [1–5].

Thin films used in microelectronics are often sandwiched between layers of dielectric insulation, resulting in films where the width is comparable to the depth. This is the case in quantum well laser diodes [6], where boundary effects are exploited for the purpose of optical confinement. However, this design has an adverse affect on the thermal transport properties and results in frequent thermal overload or "burnout." Design of these advanced microstructures requires accurate knowledge of the relevant thermophysical properties.

Mechanical properties such as the bulk modulus are also affected by physical size and deposition technique. Photoelasticity, or strain-induced effects on optical properties, is a phenomenon employed to achieve carrier confinement in quantum well and superlattice devices. Interfacial reactions between metals and substrates, such as Ni, Pt, Co, Pd, and W on GaAs/AlGaAs, create stress along the boundary, which has been demonstrated to be a controllable and reproducible method for creating carrier confinement for use in photon waveguides [7]. This requires accurate knowledge of the elastic moduli of both the substrate and the metal. As film thicknesses shrink to nanometers, the elastic moduli can be adversely affected, which is a primary concern in the design of these microstructures.

Despite the important role these thermophysical and mechanical properties play in the advancement of such devices, only a handful of investigators have reported data on the degradation of thermal diffusivity and elastic moduli. The goal of this investigation is to determine the effective bulk modulus and the effective thermal diffusivity normal to the surface of thin metal films simultaneously and in a noncontact manner. If the bulk modulus of the thin film sample does not vary, which is the case for certain thin film materials, this technique can be used to measure thin film thickness using the same data set as used for the thermal analysis [8]. This method is further demonstrated as a method for characterizing electron–phonon energy coupling phenomena.

2. BACKGROUND AND TECHNIQUE

Thermo- and piezoreflectance phenomena have been utilized for nearly two decades now for characterizing thermal and mechanical properties of highly reflecting materials [9–13]. The recent advancement of high-powered, ultrashort pulsed lasers has revolutionized the temporal resolution of these techniques, allowing for the observation of energy transport in the microscale time regime. This investigation merges two techniques

previously used independently for thin film and bulk material characterization. The first technique, termed the transient thermoreflectance (TTR) method, utilizes the inherent dependence of reflectivity on temperature characteristic of metals, semimetals, semi- and superconductors, and some dielectrics. This method was demonstrated by Paddock and Eesley [14] as an accurate means of determining thin film thermal diffusivity ($\pm 6\%$). The second technique, termed the transient piezoreflectance (TPR) [11] method relies on a similar phenomenon; however, it is used to observe the sample's reflectance response not due to a temperature rise, but due to the presence of strain induced from laser generated ultrasound. Wilcox and Calder [10] reported measuring elastic moduli with this method that were within 1–2% of published data for bulk materials.

The proposed technique for this investigation is a merger of the two cited methods. These methods were performed in a pump/probe fashion and in a simultaneous manner. This method is fully noncontact and relies on the fact that reflectivity is a function of both temperature and strain and that the material's response to each of these stimuli is on the same order of magnitude and inherently different and, thus, can be measured simultaneously without one signal drowning the other one out. This work is a continuation of previous work where the nonequilibrium heating and simultaneous extrapolation of thermal conductivity and thickness of thin film tungsten were presented. The results indicated that the thin film tungsten sample possessed a thermal conductivity that was one-third that of the bulk value. The thickness measurement relied on the assumption that the bulk modulus for thin film tungsten is the same as that of bulk tungsten, which was shown for tungsten and some other heavier metals in a report by Rouzard et al. [15]. The work presented here lifts the assumption of constant bulk modulus and directly measures this property using a known film thickness as measured by a profilometer. The experimental details are given by Hostetler et al. [8] and the related articles mentioned earlier [9–13].

3. DATA ANALYSIS

The pump/probe experimental setup described by Hostetler et al. [8] was used to monitor the change in reflectivity at the surface of a sample. The results from thin film samples show a convolution of two reflective phenomena. The measured signal shows a temporal cooling curve superimposed with surges of reflectivity induced by the ultrasonic acoustic waves.

When analyzing the TTR data, the appropriate thermal model for nonequilibrium heating in metals is termed the parabolic two-step (PTS) model. This model was developed by Anisimov et al. [16] and has been

studied extensively by Brorson et al. [17] and Qiu and Tien [18]. The PTS model differs from normal Fourier diffusion, termed the parabolic one-step (POS) model, where laser energy is assumed to be absorbed instantaneously by the lattice. The PTS assumes that the incident radiation is absorbed in a two-step process, where the laser energy is first absorbed by the electrons and then redistributed to the lattice in the second step. For a short period after the deposition of laser energy, the electrons and lattice are not in thermal equilibrium, but exchange energy through a coupling coefficient termed the electron–phonon coupling factor, denoted G. This gives rise to two temperatures present in the first few picoseconds, the electron temperature and the lattice temperature, termed T_e and T_l, respectively. The coupling factor, G, whose strength governs the rate at which energy is transferred from the "hot" electrons to the "cold" lattice, and visa versa, also affects the shape of the cooling profile long after the film is exposed to an ultrashort laser pulse, resulting in non-Fourier cooling curves.

The TTR experimental data were compared to the numerical solution of the PTS model. The data were compared only to the electron temperature, T_e, since reflection at the wavelength of 800 nm is due exclusively to electron reradiation. The model was multiplied by a factor to match the magnitudes of the data and the model. This is validated by the assumption that the change in reflectivity is related linearly to the change in temperature through a coefficient of proportionality, called the temperature coefficient. This coefficient is of the order of 10^{-5} per K for most metals and dielectrics. The largest effect of the diffusivity is in the early stages of cooling (<100 ps); therefore, the matching point was chosen to be toward the end of the cooling curve since the model and data should thermalize to the same point. Once the model was scaled, the value of thermal diffusivity was changed incrementally until the least squares minimum was found. This procedure can also be used to determine G for bulk materials if published values of thermal diffusivity are utilized.

Analysis of the TPR data involves observing propagating ultrasonic waves that are generated at the film surface and, in the thin film case, reflected off the substrate. These reflected waves create surges in the surface's reflectivity upon completing periodic round trips. Upon absorption of the laser pulse, a thermal expansion creates an isotropic stress that generates an acoustic wave of ultrasonic frequency (~ 50 GHz). This generation results in shear (transverse) and compressional (longitudinal) waves. However, by monitoring only the center of the heated region with a large pump to probe beam diameter ratio, the only acoustic wave affecting the probe's reflected intensity is the longitudinal wave. This wave propagates perpendicular to the surface along the z axis and is partially

reflected at the film/substrate interface. The resulting equation that describes this phenomenon is [11]

$$\frac{\partial^2 u}{\partial t^2} = \left(3\,\frac{1-\nu}{1+\nu}\,\frac{B}{\rho}\right)\frac{\partial^2 u}{\partial z^2} - 3\,\frac{B\beta}{\rho}\,\frac{\partial T}{\partial z} \tag{1}$$

Equation (1) is the wave equation, where the last term represents the thermal stress needed to set up an acoustic wave traveling at velocity V, where V^2 is shown to be

$$V^2 = 3\,\frac{1-\nu}{1+\nu}\,\frac{B}{\rho} \tag{2}$$

where ν is Poisson's ratio and ρ is the density. The bulk modulus, B, is calculated from Eq. (2) by measuring the acoustic velocity, V, from the observed round-trip echo time and correlating it with the known film thickness. The echo period is determined by the observation of periodic reflectivity surges that are clearly detected as shown in the results section. The accuracy of the velocity measurement is dependent solely on the film thickness measurement. Profilometers are accurate down to a few nanometers, thereby resulting in a reliable observation of the acoustic velocity. The two main sources of error in the calculation of the bulk modulus are the values of the density and Poisson's ratio used for the thin film samples. Heald and Nielsen [19] report a study utilizing X-ray reflectivity to measure density for a wide range of thin metallic films with a reported accuracy of 1%. They concluded that for most thin film metals, even as thin as 100 nm, the density is reduced by less than 10%. This is not the case in nonmetals and dielectrics, where density variances can be larger. The same is true for Poisson's ratio, where for heavier metals, the ratio can be taken as the bulk value. The accuracy of the bulk modulus measurement is estimated to be of the order of 10%.

4. BULK SAMPLE RESULTS

Before the extrapolation of thermal diffusivity for thin-film platinum was performed, a value was needed for the electron–phonon coupling factor, G. As no published values could be found for platinum, this parameter was determined experimentally. To help quantify the validity of this method, the thermoreflectance of a 99+% OFHC copper block was analyzed and compared with other reported values. By assuming the diffusivity to be that of a bulk sample, $117 \times 10^{-6}\,\mathrm{m^2 \cdot s^{-1}}$, the reflectance data were curve fit until a least-squares minimum for G was obtained. The value obtained for copper was $1.2(\pm 0.5) \times 10^{18}\,\mathrm{W \cdot m^{-3} \cdot K^{-1}}$, which is of

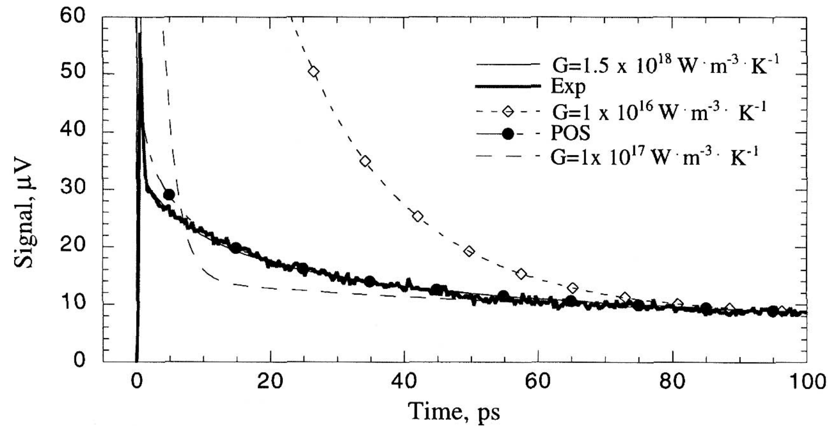

Fig. 1. Thermoreflectance response of bulk platinum and comparison to the PTS heat conduction model. The corresponding measured value for the electron-phonon coupling constant, G, is $1.5 \times 10^{18}\ \mathrm{W \cdot m^{-3} \cdot K^{-1}}$. Normal Fourier diffusion is represented by the curve entitled POS.

the same order of magnitude as that reported by Brorson et al. [17], Elsayed-Ali et al. [20], and Orlande et al. [21]. The optical and thermal properties of copper and platinum were taken from the *CRC Handbook of Tables for Applied Engineering Science* [22] and Kittel [23].

The same experimental procedure was utilized for platinum as was used for copper. The thermoreflectance response of bulk platinum is shown in Fig. 1, with the corresponding curve fit for parameter G. Also shown in Fig. 1 are other values of G to demonstrate the effect of the coupling parameter. The initial spike in the data indicates the definite presence of nonequilibrium heating. However, since the duration of the spike for most metals is near the temporal resolution of this setup ($\sim$200 fs), details of the peak are not resolved, and therefore, these data are not included in the fit. The data used in the curve fit routine were from just past the point of inflection ($\sim$2 ps) up to 100 ps. Even for low values of G ($1 \mathrm{x} 10^{16}\ \mathrm{W \cdot m^{-3} \cdot K^{-1}}$), the effect of nonequilibrium heating is seen only in the first 100 ps; therefore, only fitting to this point is valid. The value of G obtained for the platinum scan in Fig. 1 is $1.5 \times 10^{18}\ \mathrm{W \cdot m^{-3} \cdot K^{-1}}$. The average value of G for all the scans taken was $1.11(\pm 0.5) \times 10^{18}\ \mathrm{W \cdot m^{-3} \cdot K^{-1}}$.

5. THIN FILM PLATINUM RESULTS

Thin platinum films were electron beam evaporated to a thickness of 100 nm on two substrates, silicon and glass. The thickness was measured

during the deposition by a vibrating quartz crystal. To obtain a more accurate thickness measurement, the samples were measured postevaporation using a Tencor Alpha-Step 200 profilometer which has an accuracy of ± 5 nm. The profilometer results show the thickness of the Pt films to be 104 ± 5 nm for the silicon substrate and 110 ± 5 nm for the glass substrate, agreeing reasonably well with the *in situ* quartz method; however, the authors warn against relying on the quartz method due to its sensitivity to calibration. Figure 2 shows the response of thin film platinum evaporated onto a silicon substrate where the ultrasonic echoes are clearly detectable. The pulse echo period is ~ 52 ps and the resulting bulk modulus is 2.6×10^{11} N $\cdot$ m^{-2}, which agrees with the published value of 2.783×10^{11} N $\cdot$ m^{-2} within 7% [22]. This leads to the conclusion that thin film platinum's bulk modulus is very near that of bulk quantity even for thicknesses around 100 nm. The curve-fitting routine was utilized to determine the thin film thermal diffusivity, where the value of G was taken as 1.11×10^{18} W $\cdot$ m^{-3} $\cdot$ K^{-1}. This procedure yielded an effective thermal diffusivity normal to the surface of 20×10^{-6} m$^2 \cdot$ s^{-1}. The average diffusivity determined from all the thin film platinum on silicon scans was $22 \pm 2.5 \times 10^{-6}$ m$^2 \cdot$ s^{-1}, which shows a reduction from the bulk value of 25×10^6 m$^2 \cdot$ s^{-1}.

The thermoreflectance response from a thin platinum film evaporated onto a glass substrate is shown in Fig. 3. The ultrasonic generation and one echo at ~ 55 ps can barely be seen. This could be due to a difference in

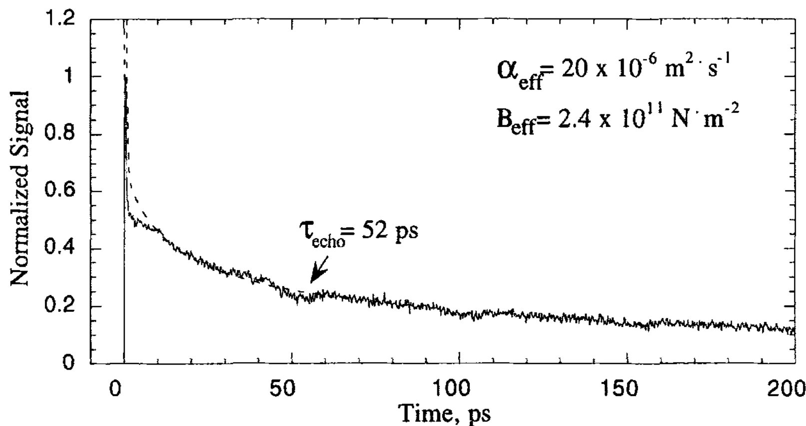

Fig. 2. Thermoreflectance response of a thin platinum film evaporated onto a silicon substrate and the corresponding curve fit using the PTS heat conduction model for effective thermal diffusivity, α_{eff}. Ultrasonic peaks, seen with a period of 52 ps, are used to calculate the effective bulk modulus, B_{eff}.

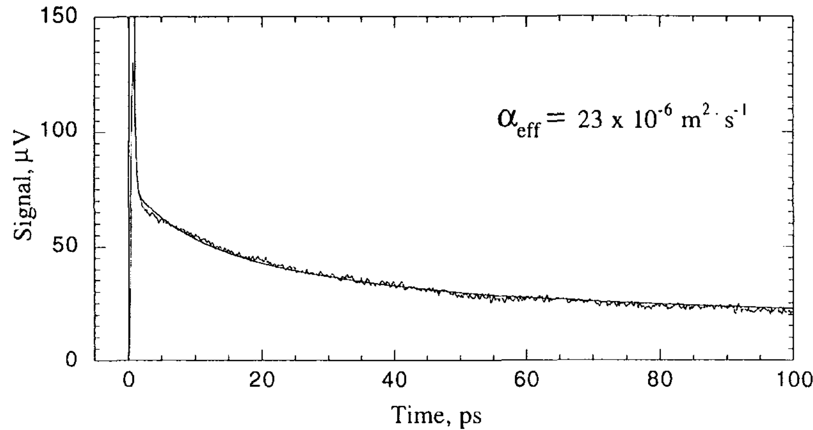

Fig. 3. Thermoreflectance response of a thin platinum film evaporated onto a glass substrate and the corresponding curve fit using the PTS heat conduction model for effective thermal diffusivity, α_{eff}. Ultrasonic generation at ~2 ps and the first echo at ~55 ps can barely be seen.

adhesion between the film and the substrate. Visual inspection of the film evaporated onto the glass shows no noticeable imperfections on the surface, while the silicon substrate shows cracks and vacant spots. The acoustic mismatch for the glass sample also results in a lower value for the acoustic reflection coefficient, which results in more transmission of the acoustic pulse into the substrate. The value of diffusivity determined for this sample is $23 \times 10^{-6}\ \text{m}^2 \cdot \text{s}^{-1}$ and the average diffusivity determined from all the scans of this sample was 21 $(\pm 2.5) \times 10^{-6}\ \text{m}^2 \cdot \text{s}^{-1}$.

6. CONCLUSIONS

Utilizing an optical pump/probe technique, evaporated thin films and bulk samples of platinum were studied to extrapolate the transient energy transfer mechanisms. The results for evaporated thin film platinum indicate that the thermal diffusivity normal to the surface is reduced by ~15% and the elastic modulus is only slightly reduced compared to literature values of bulk platinum.

Future work includes an investigation of the limitations of film thickness in this technique and a formal error analysis. This method will be demonstrated on semiconductors and dielectrics that possess refractive indices that are temperature dependent. Modeling the acoustic wave propagation for purposes of studying acoustic mismatch and adhesion between thin film and substrate interfaces is already under way.

REFERENCES

1. M. I. Flik, B. I. Choi, and K. E. Goodson, *J. Heat Transfer* **114**:666 (1992).
2. T. Q. Qiu and C. L. Tien, *Int. J. Heat Mass Transfer* **37**:2789 (1994).
3. M. I. Flik and C. L. Tien, *J. Heat Transfer* **112**:872 (1990).
4. A. B. Duncan and G. P. Peterson, *Appl. Mech. Rev.* **47**:397 (1994).
5. K. E. Goodson, O. W. Käding, M. Rösler, and R. Zachai, *J. Appl. Phys.* **77**:1385 (1995).
6. P. M. Norris, G. Chen, and C. L. Tien, *Int. J. Heat Mass Transfer* **37**:9 (1994).
7. Q. Z. Liu, F. Deng, L. S. Yu, Z. F. Guan, S. A. Pappert, P. K. L. Yu, and S. S. Lau, *J. Appl. Phys.* **78**:236 (1995).
8. J. L. Hostetler, A. N. Smith, and P. M. Norris, *Micro. Thermophys. Eng.* **1**:237 (1997).
9. R. M. White, *J. Appl. Phys.* **34**:3559 (1962).
10. W. W. Wilcox and C. A. Calder, *Instrum. Tech.* **25**:63 (1978).
11. C. Thomsen, H. T. Grahn, H. J. Maris, and J. Tauc, *Phys. Rev. B* **34**:4129 (1986).
12. H. T. Grahn, H. J. Maris, and J. Tauc, *IEEE J. Quant. Elect.* **25**:2562 (1989).
13. C. B. Scruby and L. E. Drain, *Laser Ultrasonics* (IOP, Bristol, 1990).
14. C. A. Paddock and G. L. Eesley, *J. Appl. Phys.* **60**:285 (1986).
15. A. Rouzaud, E. Barbier, J. Ernoult, and E. Quesnel, *Thin Solid Films* **270**:270 (1995).
16. S. I. Anisimov, B. L. Kapeliovich, and T. L. Perel'man, *Sov. Phys. JETP* **39**:375 (1974).
17. S. D. Brorson, A. J. Kazeroonian, S. Moodera, D. W. Face, T. K. Cheng, E. P. Ippen, M. S. Dresselhaus, and G. Dresselhaus, *Phys. Rev. Lett.* **64**:2172 (1990).
18. T. Q. Qiu and C. L. Tien, *J. Heat Transfer* **115**:835 (1993).
19. S. M. Heald and B. Nielsen, *J. Appl. Phys.* **72**:4669 (1992).
20. H. E. Elsayed-Ali, T. B. Norris, M. A. Pessot, and G. A. Mourou, *Phys. Rev. Lett.* **58**:1212 (1987).
21. H. R. B. Orlande, M. N. Ozisik, and D. Y. Tzou, *J. Appl. Phys.* **78**:1843 (1995).
22. R. E. Bolz and G. L. Tuve, *CRC Handbook of Tables for Applied Engineering Science*, 2nd ed. (CRC Press, Boca Raton, FL, 1976).
23. C. Kittel, *Introduction to Solid State Physics*, 7th ed. (Wiley, New York, 1996).